PHYSICAL REVIEW D **96,** 094001 (2017)

Charge distribution of $d^*(2380)$

Yubing Dong,[1,2,3] Fei Huang,[3] Pengnian Shen,[4,1,2] and Zongye Zhang[1,2,3]

[1]*Institute of High Energy Physics, Chinese Academy of Sciences, Beijing 100049, China*
[2]*Theoretical Physics Center for Science Facilities (TPCSF), CAS, Beijing 100049, China*
[3]*School of Physical Sciences, University of Chinese Academy of Sciences, Beijing 101408, China*
[4]*College of Physics and Technology, Guangxi Normal University, Guilin 541004, China*

(Received 8 July 2017; published 8 November 2017)

Based on a chiral constituent quark model, we calculate the charge distributions of $d^*(2380)$. We consider the existence of two different interpretations of the d^*: a compact structure in the two-coupled-channel ($\Delta\Delta + CC$) approximation, and a resonant structure of $D_{12}\pi$. We calculate the charge distribution of the d^* with a compact structure, and we also roughly estimate the charge distribution for a $D_{12}\pi$ structure on the same base. The result shows that there is a remarkable difference in the charge distributions of the two structural pictures. Therefore, we expect that future experiments may provide a clear signal for the d^* structure.

DOI: 10.1103/PhysRevD.96.094001

I. INTRODUCTION

$d^*(2380)$ is a new resonance recently observed by the CELSIUS/WASA and WASA@COSY collaborations [1,2]. It was found in the analysis of the double pionic fusion channels $pn \to d\pi^0\pi^0$ and $pn \to d\pi^+\pi^-$ when the ABC effect [3] and the analyzing power A_y of the neutron-proton scattering data were studied. It is argued that the observed structure cannot be simply understood by either the intermediate Roper excitation contribution or the t-channel $\Delta\Delta$ process. References [1,2] proposed the assumption of there existing a d^* resonance whose quantum number, mass, and width are $I(J^P) = 0(3^+)$, $M \approx 2370$ MeV, and $\Gamma \approx 70$ MeV, respectively (see also their recent paper [4]; the averaged mass and width are $M \approx 2375$ MeV and $\Gamma \approx 75$ MeV, respectively). Since the baryon number of the d^* is 2, it would be treated as a dibaryon, and could be explained by either "an exotic compact particle" or "a hadronic molecule state" [5]. Moreover, since the observed mass of the d^* is about 80 MeV below the $\Delta\Delta$ threshold and about 70 MeV above the $\Delta\pi N$ threshold, the threshold (or cusp) effect may not be as significant as that in the XYZ particles (see the review of XYZ particles in Ref. [6], for example). Thus, understanding the internal structure of the d^* would be of great interest.

The existence of such a nontrivial six-quark configuration with $I(J^P) = 0(3^+)$ (called d^* lately) has triggered great attention and has intensively been studied in the literature even before the COSY's discovery [7–15]. In fact, after the experimental observation of the d^*, there are three main types of model explanations for its nature in the market. The first type regards it as a $\Delta\Delta$ bound state. The typical work is a calculation in terms of the chiral $SU(2)$ quark model in Refs. [16,17]. The second type asserts that the d^* has a resonant structure of $D_{12}\pi$ [18–24] with a resonant pole around $(2363 \pm 20) + i\,(65 \pm 17$ MeV). In this model, D_{12} is an $N\Delta$ resonance with an S-matrix pole positioned at $2159 - i70$ MeV obtained by solving $NN\pi$ Faddeev equations [18–21]. The third type, following our previous prediction [15], suggests a dominant hexaquark structure for the d^*, with a mass of about 2380–2414 MeV and a width of about 71 MeV [25–29]. Most recently, another $\Delta\Delta - D_{12}\pi$ mixed model is also proposed, in which the fraction of the $\Delta\Delta$ component is about $5/7$ [30]. From the above mentioned model results, one has the following observations: (1) All proposed models can almost reproduce the observed mass of the d^*. (2) Only the last two models provide a total width for the d^* which is compatible with the observed data. Moreover, in terms of the third (hexaquark-dominant) model, the predicted width of the single-pion decay mode of $d^* \to NN\pi$ is about 1 MeV, which is small compared with its double-pion decay widths [29]. Here, we particularly mention that this value is much narrower than the width for a pure $D_{12}\pi$ structure with the second approach, but it is not contradictory to experimental observation [31] or the result from the $\Delta\Delta$-$D_{12}\pi$ mixed model [30] found very recently. Anyway, all the outcomes from the third model support the idea that the d^* is probably a compact six-quark-dominated exotic state due to its large CC component, which has also been pointed out by Bashkanov, Brodsky, and Clement [32]. Therefore, the model decay width of the $d^* \to NN\pi$ process might help us to understand its structure; in other words, the width might be sensitive to the structure of the d^*. However, to ultimately pin down its structure, more discriminating observables and processes should still be investigated. A general review on the dibaryon studies can be found in Ref. [33].

It is known that the electromagnetic probe is one of the most useful tools to test the internal structure of a complicated system. For example, the electromagnetic form factors of the nucleon show its charge and magnetic distributions. The slopes of the charge and magnetic

distributions at the origin give the charge and magnetic radii of the system. The precise measurement of the charge radius of the proton provides criteria for different model calculations. For the spin-1 particle, like a deuteron or a ρ meson, the charge, magnetic, and quadrupole form factors tell us its intrinsic structures as well, like charge and magnetic distributions and the quadrupole deformation of the system. Therefore, the form factors of the d^*—for instance, the charge distribution—might also be a discriminating quantity for its structure. In particular, if the d^* has a considerably large hidden color component (HCC), such a component does not contribute to its hadronic decays in the leading-order calculation, but plays a rather important role in its charge distribution calculation. Therefore, the charge distribution of the d^* reveals the effect of HCC in it. On the other hand, because the chiral $SU(3)$ constituent quark model with fixed model parameters can well explain the data of the baryon ground states, the nucleon-nucleon scattering phase shifts and nucleon-hyperon cross sections, the binding energy of the deuteron, and even the H particle in its present experimental status, etc. [25,26,34–38], the model has certain power of prophecy. Therefore, in this work, the charge distribution of the new resonance $d^*(2380)$ will be discussed on the base of the chiral $SU(3)$ constituent quark model with a single $\Delta\Delta$ structure or a coupled $\Delta\Delta + CC$ structure. For comparison, the charge distribution of the d^* with a resonant structure of $D_{12}\pi$ is also calculated on the base of the same quark model. Now, since the $d^*(2380)$ is a spin-3 particle, it has $2S+1=7$ form factors. A detailed discussion of all seven form factors is beyond the scope of this work and will be given elsewhere. Here we only concentrate on its charge distribution and the charge radius of the $d^*(2380)$ in the two scenarios.

This paper is organized as follows: In Sec. II, a brief discussion about the electromagnetic form factors of the particles with spin 1/2, spin 1, and spin 3 will be shown. An explicit calculation of the charge distribution of the d^* with two scenarios is given in Sec. III. Section IV is devoted to a short summary.

II. ELECTROMAGNETIC FORM FACTORS

The study of the electromagnetic form factors of the nucleon (spin-1/2) is of great interest, because it can tell us information about the charge and magnetic distributions of a nucleon. In the one-photon approximation, the electromagnetic current of a nucleon is

$$\langle N(p')|J_N^\mu|N(p)\rangle = \bar{U}_N(p')\left[F_1(Q^2)\gamma^\mu + i\frac{\sigma^{\mu\nu}q_\nu}{2M_N}F_2(Q^2)\right]U(p), \quad (1)$$

where M_N is the nucleon mass, $q=p'-p$ is the momentum transfer, $Q^2=-q^2$, and $F_1(Q^2)$ and $F_2(Q^2)$ are the Dirac and Pauli form factors, respectively. These two form factors relate to Sach's form factors, the electric and magnetic form factors, as

$$G_E(Q^2) = F_1(Q^2) - \eta F_2(Q^2),$$
$$G_M(Q^2) = F_1(Q^2) + F_2(Q^2), \quad (2)$$

with $\eta = Q^2/4M_N^2$. The normalization conditions of the two form factors for the proton and neutron are $G_E^p(0)=1$ and $G_E^n(0)=0$, and $G_M^p=2.79$ and $G_M^n=-1.91$, respectively. Then, Eq. (1) reduces to [39–44]

$$\langle N(p')|J_N^\mu|N(p)\rangle = \frac{1}{1+\eta}\bar{u}_N(p',s')\left[(1+\eta)G_M\gamma^\mu - \frac{G_M-G_E}{2M_N}P^\mu\right]u_N(p,s), \quad (3)$$

where $P=p'+p$. In the Breit frame, we have $q^\mu=(0,\vec{q})$, $p'^2=p^2=M_N^2$, $\vec{p}=-\vec{p}'=-\frac{1}{2}\vec{q}$, and $p_0=p_0'=E=M_N(1+\eta)^{1/2}$. Then, the time and space components of the nucleon electromagnetic current in Eq. (1) are proportional to particular combinations of the Dirac and Pauli form factors that can be interpreted as Fourier transforms of electric charge and magnetization spatial densities of the nucleon [39–44]. We have

$$\langle N(\vec{q}/2)|J_N^0|N(-\vec{q}/2)\rangle = (1+\eta)^{-1/2}\chi_{s'}^+\chi_s G_E(Q^2),$$
$$\langle N(\vec{q}/2)|\vec{J}_N|N(-\vec{q}/2)\rangle = (1+\eta)^{-1/2}\chi_{s'}^+\frac{\vec{\sigma}\times\vec{q}}{2M_N}\chi_s G_M(Q^2). \quad (4)$$

Clearly, the matrix element of J_N^0 is directly related to the electric form factor $G_E(Q^2)$ and to the diagonal matrix element without spin flip, and by employing the Breit reference frame, one may easily sort out the charge form factor of the nucleon.

A spin-1 particle, like a deuteron [45–49] or a ρ meson [50–53], contains three form factors. In the one-photon approximation, the electromagnetic current is

$$J_{jk}^\mu(p',p) = \epsilon_j'^{*\alpha}(p')S_{\alpha\beta}^\mu\epsilon_k^\beta(p), \quad (5)$$

where ϵ^α and ϵ'^β stand for the polarization vectors of the incoming and outgoing deuterons, i and k are the polarizations of the two deuterons, and

$$S_{\alpha\beta}^\mu = -\left[G_1(Q^2)g_{\alpha\beta} - G_3(Q^2)\frac{Q_\alpha Q_\beta}{2M_D^2}\right]P^\mu - G_2(Q^2)(Q_\alpha g_\beta^\mu - Q_\beta g_\alpha^\mu), \quad (6)$$

where $P=p'+p$. The three form factors $G_{1,2,3}(Q^2)$ relate to the charge $G_C(Q^2)$, magnetic $G_M(Q^2)$, and quadrupole form factors $G_Q(Q^2)$ as

$$G_C(Q^2)=G_1(Q^2)+\frac{2}{3}\eta_D G_Q(Q^2),\quad G_M(Q^2)=G_2(Q^2), \tag{7}$$

$$G_Q(Q^2)=G_1(Q^2)-G_2(Q^2)+(1+\eta_D)G_3(Q^2), \tag{8}$$

with $\eta_D=Q^2/4M_D^2$ and M_D the deuteron mass. The charge, magnetic, and quadrupole form factors are normalized to $G_C(0)=1$, $G_M(0)=\frac{M_D}{M_N}\mu_d=1.714$, and $G_Q(Q^2)=M_D^2Q_d=25.83$, respectively. One may also extract the charge form factor of the deuteron $G_C(Q^2)$ by directly calculating the matrix element $\frac{1}{3}\sum_\lambda\langle p',\lambda|J^0|p,\lambda\rangle$ in the Breit reference frame.

For the $d^*(2380)$ particle, since its spin is 3, it has $2S+1=7$ form factors. Its field can be expressed as $\epsilon_{\alpha\beta\gamma}$, a rank-3 tensor, which is traceless. Clearly, $\epsilon_{\alpha\alpha\beta}=0$, $\epsilon_{\alpha\beta\gamma}=\epsilon_{\beta\alpha\gamma}$, and $p^\alpha\epsilon_{\alpha\beta\gamma}=0$. Moreover, we have (in analogy to the spin-2 case in Ref. [54]),

$$\sum_{\rm pol}\epsilon_{\mu\nu\sigma}\epsilon^*_{\alpha\beta\gamma}=\frac{1}{6}[\tilde g_{\mu\alpha}(\tilde g_{\nu\beta}\tilde g_{\sigma\gamma}+\tilde g_{\nu\gamma}\tilde g_{\sigma\beta})+\tilde g_{\mu\beta}(\tilde g_{\nu\alpha}\tilde g_{\sigma\gamma}+\tilde g_{\nu\gamma}\tilde g_{\sigma\alpha})+\tilde g_{\mu\gamma}(\tilde g_{\nu\alpha}\tilde g_{\sigma\beta}+\tilde g_{\nu\beta}\tilde g_{\sigma\alpha})]$$
$$-\frac{1}{15}[\tilde g_{\mu\nu}(\tilde g_{\sigma\alpha}\tilde g_{\beta\gamma}+\tilde g_{\sigma\beta}\tilde g_{\alpha\gamma}+\tilde g_{\sigma\gamma}\tilde g_{\alpha\beta})+\tilde g_{\mu\sigma}(\tilde g_{\nu\alpha}\tilde g_{\beta\gamma}+\tilde g_{\nu\beta}\tilde g_{\alpha\gamma}+\tilde g_{\nu\gamma}\tilde g_{\alpha\beta})+\tilde g_{\nu\sigma}(\tilde g_{\mu\alpha}\tilde g_{\beta\gamma}+\tilde g_{\mu\beta}\tilde g_{\alpha\gamma}+\tilde g_{\mu\gamma}\tilde g_{\alpha\beta})], \tag{9}$$

with

$$\tilde g_{\mu\nu}=-g_{\mu\nu}+\frac{p_\mu p_\nu}{M^2}, \tag{10}$$

where M is the mass of the d^*.

In the one-photon exchange approximation, the general form of the electromagnetic current of the 3^+ particle is

$$\mathcal{J}^\mu=(\epsilon^*)^{\alpha'\beta'\gamma'}(p')\mathcal{M}^\mu_{\alpha'\beta'\gamma',\alpha\beta\gamma}\epsilon^{\alpha\beta\gamma}(p), \tag{11}$$

and the matrix element

$$\begin{aligned}\mathcal{M}^\mu_{\alpha'\beta'\gamma',\alpha\beta\gamma}=&[G_1(Q^2)\mathcal{P}^\mu[g_{\alpha'\alpha}(g_{\beta'\beta}g_{\gamma'\gamma}+g_{\beta'\gamma}g_{\gamma'\beta})+\text{permutations}]\\&+G_2(Q^2)\mathcal{P}^\mu[q_{\alpha'}q_\alpha[g_{\beta'\beta}g_{\gamma'\gamma}+g_{\beta'\gamma}g_{\gamma'\beta}]+\text{permutations}]/(2M^2)\\&+G_3(Q^2)\mathcal{P}^\mu[q_{\alpha'}q_\alpha q_{\beta'}q_\beta g_{\gamma'\gamma}+\text{permutations}]/(4M^4)\\&+G_4(Q^2)\mathcal{P}^\mu q_{\alpha'}q_\alpha q_{\beta'}q_\beta q_{\gamma'}q_\gamma/(8M^6)+G_5(Q^2)[(g^\mu_{\alpha'}q_\alpha-g^\mu_\alpha q_{\alpha'})(g_{\beta'\beta}g_{\gamma'\gamma}+g_{\beta'\gamma}g_{\beta'\gamma})+\text{permutations}]\\&+G_6(Q^2)[(g^\mu_{\alpha'}q_\alpha-g^\mu_\alpha q_{\alpha'})(q_{\beta'}q_\beta g_{\gamma'\gamma}+q_{\gamma'}q_\gamma g_{\beta'\beta}+q_{\beta'}q_\gamma g_{\gamma'\beta}+q_{\gamma'}q_\beta g_{\gamma\beta'})+\text{permutations}]/(2M^2)\\&+G_7(Q^2)[(g^\mu_{\alpha'}q_\alpha-g^\mu_\alpha q_{\alpha'})q_{\beta'}q_\beta q_{\gamma'}q_\gamma+\text{permutations}]/(4M^4)],\end{aligned} \tag{12}$$

where $\mathcal{P}=p'+p$, and $G_{1,2,3,4,5,6,7}(Q^2)$ are the seven elastic form factors. The gauge invariant condition

$$q_\mu\mathcal{M}^\mu_{\alpha'\beta'\gamma',\alpha\beta\gamma}=0 \tag{13}$$

is fulfilled, as well as the time-reversal invariance. In general, the combinations of the above seven elastic form factors $G_{1,2,\ldots,7}(Q^2)$ can give the physical form factors of the d^* such as the charge, magnetic, quadrupole, and octupole, as well as other higher-order multiple form factors. However, those combinations are unknown. Moreover, the normalizations of all the form factors are unknown as well, except for the charge form factor of $G_c(0)=1$.

In analogy to the spin-1/2 nucleon and spin-1 deuteron cases, we assume that the charge distribution of the spin-3 particle, $d^*(2380)$, is also directly related to the spin nonflip matrix element of J^0 which is the time component of the current J^μ, and working in the Breit frame, we may untangle the complex relations of the seven elastic form factors and pick up the charge distribution like the cases of the nucleon and spin-1 particle. According to this hypothesis, the charge distribution of the $d^*(2380)$, which is a six-quark system, can approximately be extracted from the spin nonflip matrix element of J^0 in the Breit frame, as well in the form of

$$G_E^{d^*}(Q^2)=\frac{1}{7}\sum_{m_{d^*}=-3}^{3}\langle p',m_{d^*}|J^0|p,m_{d^*}\rangle, \tag{14}$$

where the quark-quark-photon current reads

$$J^0=\sum_{i=1}^{6}e_i\bar q_i\gamma^0 q_i=\sum_{i=1}^{6}j_i^0. \tag{15}$$

It should be mentioned that although a detailed study of all seven elastic form factors should be carried out, it is beyond the scope of this paper, and it will be done in the future.

III. CALCULATIONS OF THE d^* CHARGE DISTRIBUTION IN TWO SCENARIOS

Two extreme pictures for the d^* structure are a compact hexaquark-dominated state [25–29] and a $\Delta N\pi$ (or $D_{12}\pi$) state. Since these two structures have same quantum numbers, the observed state might be of their mixture, namely an extended structure [30]. If the former structure has a large fraction, the system is more like a compact hexaquark-dominated state, and otherwise like a quasimolecular state. We believe that the future measured charge distribution of the d^* would help us to figure out the fractions of these two structures in it, and consequently to obtain its structure information. Therefore, in this paper, we would concentrate on the charge distribution of the $d^*(2380)$, and show how the charge distribution curve goes in these two extreme cases, scenarios A and B.

A. Scenario A: Hexaquark-dominant structure

We first consider the charge distribution of the $d^*(2380)$ with a hexaquark-dominated structure. As mentioned in Refs. [25–27], our model wave function for the $d^*(2380)$ is obtained by dynamically solving the bound-state RGM (resonating group method) equation of the six-quark system in the framework of our extended chiral $SU(3)$ quark model [34,35], and then successively projecting the solution onto the inner cluster wave functions of the $\Delta\Delta$ and CC channels. The resultant wave function of the d^* can finally be abbreviated to a form of

$$\begin{aligned}|\Psi_{d^*(2380)}\rangle &= \alpha|\Delta\Delta\rangle_{(SI)=(30)} + \beta|CC\rangle_{(SI)=(30)} \\ &= |[\phi_\Delta(\vec{\xi}_1,\vec{\xi}_2)\phi_\Delta(\vec{\xi}_4,\vec{\xi}_5)\chi_{\Delta\Delta}(\vec{r})\zeta_{\Delta\Delta} \\ &\quad + \phi_C(\vec{\xi}_1,\vec{\xi}_2)\phi_C(\vec{\xi}_4,\vec{\xi}_5)\chi_{CC}(\vec{r}))\zeta_{CC}]\rangle_{(SI)=(30)},\end{aligned} \tag{16}$$

where α and β are the fractions of the $\Delta\Delta$ and CC components in the $d^*(2380)$, ϕ_Δ and ϕ_C denote the inner cluster wave functions of Δ and C (color-octet particle) in the coordinate space, $\chi_{\Delta\Delta}$ and χ_{CC} represent the channel wave functions in the $\Delta\Delta$ and CC channels (in the single $\Delta\Delta$ channel case, the CC component is absent), and $\zeta_{\Delta\Delta}$ and ζ_{CC} stand for the spin-isospin wave functions in the hadronic degrees of freedom in the corresponding channels, respectively [25,26]. It should be specially mentioned that in such a d^* wave function, two channel wave functions are orthogonal to each other and contain all the effects of totally antisymmetrized wave functions of quarks implicitly [25,26] (refer also to the Appendix for more detailed information).

Unlike in the calculations of the decay processes of $d^* \to d\pi\pi$, $d^* \to NN\pi\pi$, and $d^* \to NN\pi$, where the CC component does not contribute to the widths, here in the calculation of the charge distribution of the d^*, both the CC and $\Delta\Delta$ components contribute. Considering that the Δ and C are antisymmetric, the charge distribution is

$$\begin{aligned}G_E^{(A)}(Q^2) &= \frac{1}{7}\sum_{m_{d^*}}\langle d^*(\mathcal{P}', m_{d^*})|\sum_{i=1}^{6} j_i^0|d^*(\mathcal{P}, m_{d^*})\rangle \\ &= \frac{3}{7}\sum_{m_{d^*}}\langle d^*(\mathcal{P}', m_{d^*})|(e_3 j_3^0 + e_6 j_6^0)|d^*(\mathcal{P}, m_{d^*})\rangle,\end{aligned} \tag{17}$$

where the superscript (A) stands for scenario A, $\vec{\mathcal{P}}' - \vec{\mathcal{P}} = \vec{q}$, $Q^2 = -q^2 = \vec{q}^2$, and $e_{3,6} = \frac{1}{6} + \frac{\tau_{3,6}^z}{2}$. Then

$$G_E^{(A)}(Q^2) = 3[\alpha^2(I_3^\Delta + I_6^\Delta)\mathcal{O}_\Delta\mathcal{O}_{\chi_\Delta} + \beta^2(I_3^C + I_6^C)\mathcal{O}_C\mathcal{O}_{\chi_C}], \tag{18}$$

where $\mathcal{O}_{\Delta,C}$ denote the overlaps of the wave functions of the third quark (or sixth quark) which is bombarded by the photon in the Δ and C systems, and $\mathcal{O}_{\chi_\Delta}$ and $\mathcal{O}_{\chi_C}$ represent the contributions from the $\Delta\Delta$ and CC channel wave functions, respectively. $I_{3,6}^{\Delta,C}$ can be calculated by

$$\begin{aligned}I_{3,6}^\Delta &= {}_{(I,I_z)}\langle\Delta\Delta|e_{3,6}|\Delta\Delta\rangle_{(I,I_z)}, \\ I_{3,6}^C &= {}_{(I,I_z)}\langle CC|e_{3,6}|CC\rangle_{(I,I_z)}.\end{aligned} \tag{19}$$

Finally, one obtains

$$G_E^{(A)}(Q^2) = \left[\alpha^2\exp\left[-\frac{b_\Delta^2\vec{q}^2}{6}\right]\mathcal{O}_{\chi_\Delta} + \beta^2\exp\left[-\frac{b_c^2\vec{q}^2}{6}\right]\mathcal{O}_{\chi_c}\right], \tag{20}$$

where $b_{\Delta,C}$ are the size parameters of the Δ and C systems. As has been discussed explicitly in Ref. [27], for easily making analytic derivation, the channel wave function for the $\Delta\Delta$ channel obtained by solving the bound-state RGM equation is fitted by

$$\chi(r)_{\Delta\Delta} = \sum_{m=1}^{4}\frac{c_m}{\sqrt{4\pi}}\exp\left(-\frac{r^2}{2b_m^2}\right), \tag{21}$$

where c_m and b_m can be determined in the fitting process. Thus,

$$\mathcal{O}_{\chi_\Delta}(Q^2) = \langle \chi_{\Delta\Delta}(\vec{k}+\vec{q}/2)|\chi_{\Delta\Delta}(\vec{k})\rangle = \sum_{mn} c_m c_n \frac{b_m^3 b_n^3}{4\pi}\left(\frac{2\pi}{b_m^2+b_n^2}\right)^{3/2} \times \exp\left[-\frac{b_m^2 b_n^2}{8(b_m^2+b_n^2)}\vec{q}^2\right]. \quad (22)$$

For the CC component, the channel wave function is dominated by the single S-wave Gaussian function

$$\chi_{CC}(r) = (b_c^r\sqrt{\pi})^{-3/2}\exp[-r^2/2(b_c^r)^2]. \quad (23)$$

Similarly, the contribution from the CC component can be calculated by

$$\mathcal{O}_{\chi_C}(Q^2) = \langle \chi_{CC}(\vec{k}+\vec{q}/2)|\chi_{CC}(\vec{k})\rangle = \exp\left[-\frac{(b_c^r)^2}{16}\vec{q}^2\right]. \quad (24)$$

B. Scenario B: $D_{12}\pi$ structure

Now, we calculate the charge distribution of a d^* which is assumed to have a $D_{12}\pi$ structure. We should be aware that $D_{12}\pi$ in the isospin space should be decomposed as

$$|d^*\rangle = \frac{1}{\sqrt{3}}[D_{12}(I_z=1)\pi^- - D_{12}(I_z=0)\pi^0 + D_{12}(I_z=-1)\pi^+]. \quad (25)$$

The Jacobi momenta of the $D_{12}-\pi$ system are

$$\vec{\mathcal{P}} = \vec{p}_\pi + \vec{p}_{D_{12}}, \quad \vec{\tilde{q}} = \frac{m_\pi \vec{p}_{D_{12}} - M_{D_{12}}\vec{p}_\pi}{m_\pi + M_{D_{12}}} = a\vec{p}_{D_{12}} - a'\vec{p}_\pi, \quad (26)$$

where $\vec{p}_\pi$ and $\vec{p}_{D_{12}}$ are the momenta of π and D_{12}, respectively, and $\vec{\tilde{q}}$ stands for the relative momentum between the two systems. From the above equation, one sees that the bombarding effect of the photon on the relative momentum $\vec{\tilde{q}}$ is much smaller in the case where D_{12} is stricken than that in the case where π is hit. This is because of the factors of $a = m_\pi/(M_{D_{12}}+m_\pi)\sim 6/100$ and $a' = 1-a = M_{D_{12}}/(M_{D_{12}}+m_\pi)\sim 94/100$.

From Sec. III A, one sees that the charge distribution of a six-quark system comes from three factors: one is related to the isospin part, and the other two are the parts related to the wave functions of the constituents in the system and to the relative wave function between the constituents. Similarly, the contributions to the charge distribution of the d^* with a $D_{12}\pi$ structure should come from the D_{12}, the π, and from the relative wave function between D_{12} and π,

$$G^{(B)}_{E,m_{d^*}}(Q^2) = \frac{1}{3}\left[\sum_{m_t,m_l} C^{J_{d^*}m_{d^*}}_{s_{D_{12}}m_{D_{12}}lm_l}(\mathcal{G}_E^{D_{12}}(m_t)\mathcal{O}^{\rm rel}_{D_{12}}(aq;m_l) + \hat{\mathcal{S}}_\pi\mathcal{O}^{\rm rel}_\pi(a'q;m_l))\right], \quad (27)$$

where $\mathcal{G}_E^{D_{12}}(m_t)$ and $\hat{\mathcal{S}}_\pi$ denote the charge distributions of D_{12} and π, respectively, and $\mathcal{O}^{\rm rel}_{D_{12},\pi}$ describes the contribution of the relative wave function between D_{12} and π, with the subscript D_{12} (or π) representing the case where D_{12} (or π) is hit by the photon.

We first consider the charge distribution of the D_{12}. Assuming the D_{12} to be a bound state of the Δ and N, this distribution can also be obtained straightforwardly by calculating three factors: the isospin part, $\hat{\mathcal{E}}^{m_t}_{3,6}$; the part related to the wave function of the Δ (N), $\hat{\mathcal{S}}_{N,\Delta}$; and the part related to the relative wave function between the Δ and N, $\mathcal{O}_{\chi_{N\Delta}}$. The explicit form of the charge distribution can be written as

$$\mathcal{G}_E^{D_{12}}(m_t) = 3[\hat{\mathcal{S}}_N\hat{\mathcal{E}}_3^{m_t} + \hat{\mathcal{S}}_\Delta\hat{\mathcal{E}}_6^{m_t}]\times\mathcal{O}_{\chi_{N\Delta}}, \quad (28)$$

where m_t stands for the third component of the isospin of D_{12},

$$\hat{\mathcal{E}}_3^{m_t} = \langle 1,m_t|e_3|1,m_t\rangle = \frac{1}{6}\left(\frac{1}{2},1,\frac{3}{2}\right), \quad (m_t=1,0,-1),$$
$$\hat{\mathcal{E}}_6^{m_t} = \langle 1,m_t|e_6|1,m_t\rangle = \frac{1}{6}\left(\frac{7}{2},1,-\frac{3}{2}\right), \quad (m_t=1,0,-1), \quad (29)$$

$$\hat{\mathcal{S}}_{N,\Delta}(Q^2) = \exp\left[-\frac{b_{N,\Delta}^2\vec{q}^2}{6}\right], \quad (30)$$

and

$$\mathcal{O}_{\chi_{N\Delta}}(Q^2) = \langle\chi_{N\Delta}(\vec{k}+\vec{q}/2)|\chi_{N\Delta}(\vec{k})\rangle. \quad (31)$$

To calculate Eq. (28), we need the relative wave function $\chi_{N\Delta}$ between Δ and N. To be consistent with the frame in the above subsection, we calculate the wave function of D_{12} in the $N\Delta$ system with the quantum numbers of $I=1$ and $S=2$ by using our chiral $SU(3)$ constituent quark model with a set of reasonable model parameters. The obtained mass of the D_{12} is about $M_N+M_\Delta-\epsilon\sim$ (2167–2171) MeV (ϵ is the binding energy), which is very close to the threshold of the $N\Delta$ of 2171 MeV and compatible with the theoretical results of 2171 MeV from other quark model calculation [55], and even that of 2159 MeV from a $N-N-\pi$ three-body calculation [18,19]: namely, all theoretical predictions for the binding energy of the D_{12} tend to a value of (0–12) MeV. It should be mentioned that although we can produce a mass of about

2151 MeV, according to the experimental hint [56,57], by adjusting our model parameters in the seemingly reasonable regions, the resultant binding energy for the deuteron would be very large, which implies that the larger binding energy for the D_{12} can only be a reference. The discrepancy between the theoretical prediction and the experimental measurement indicates that the observed D_{12} might not be a pure $N\Delta$ state; its more complex structure should be carefully investigated. Now, as a crude estimation in the preliminary study, we temporarily assume that the D_{12} has a simple $N\Delta$ structure with a mass in the range of 2153–2171 MeV. Then, by solving the bound-state RGM equation, one can obtain the relative wave function between the N and Δ similar to the form of Eq. (A10).

Now, we consider the contribution from the pion. For simplicity, we may take a phenomenological monopole parametrization of the pion charge distribution [58] as an approximation.

Finally, we calculate the contribution from the relative wave function between the D_{12} and π. Since the quantum numbers $I(J^P)$ of the D_{12}, π, and d^* are $1(2^+)$, $1(0^-)$, and $0(3^+)$, respectively, from the conservations for spin, isospin, and parity, the relative wave function between the D_{12} and π must be at least a P-wave. Therefore, one can take a relative P-wave function with various size parameters as a test wave function to see how the charge distribution of the d^* goes. A typical form of such a wave function can be written as

$$\chi_{D_{12}\pi}(\vec{\tilde{q}};m_l)=\frac{\sqrt{2}b^{5/2}}{\pi^{3/4}}\mathcal{Y}_{1m_l}(\Omega_{\tilde{q}})\exp(-\tilde{b}^2\vec{\tilde{q}}^2/2), \quad (32)$$

where $\mathcal{Y}_{1,m_l}(\Omega_{\tilde{q}})$ is a so-called solid harmonics with $(l,m_l)=(1,m_l)$, and $\tilde{b}$ denotes the size parameter for the relative motion between the D_{12} and π. Then the contribution of such a relative wave function can be calculated by

$$\mathcal{O}^{\rm rel}_{D_{12}(\pi)}(\vec{\tilde{k}};m_l)=\langle\chi_{D_{12}\pi}(\vec{\tilde{q}}+\vec{\tilde{k}};m_l)|\chi_{D_{12}\pi}(\vec{\tilde{q}};m_l)\rangle, \quad (33)$$

where $\vec{\tilde{k}}$ stands for the change of the relative momentum $\vec{\tilde{q}}$ when the photon hits the D_{12} (or π). The result shows that when $\tilde{b}$ takes a value in a rather large region—for instance, from 0.6–6 fm—the obtained charge distribution of the d^* only has a very small variation. Therefore, as a rough estimation in our preliminary study for comparison, we can take a single P-wave function with a size parameter in the above mentioned region as the relative wave function without strictly solving the $D_{12}\pi$ system but still keeping the general character of such a structure.

It should be stressed that the pion contributions from the first and the third terms of Eq. (25) cancel each other, since we consider the matrix element weighted by the charge. Moreover, the one from the second term vanishes as well, since it relates to the neutron π. Therefore, our estimated charge distribution of the $d^*(2380)$ in this scenario is irrelevant to the explicit form of the pion charge form factor, and it is only due to the contributions by the D_{12} and by the relative motion between the D_{12} and π. Averaging over the initial states with various magnetic quantum numbers of the d^*, one finally obtains the charged distribution of the d^* in the $D_{12}\pi$ scenario as

$$G_E^{(B)}(Q^2)=\frac{1}{2}f_{D_{12}}(a^2\vec{q}^2)\times\mathcal{O}_{\chi_{N\Delta}}[\exp(-b_N^2\vec{q}^2/6)+\exp(-b_\Delta^2\vec{q}^2/6)], \quad (34)$$

where

$$f_{D_{12}}(a^2\vec{q}^2)=\left(1-\frac{a^2\tilde{b}^2}{5}q^2\right)\exp\left[-\frac{a^2\tilde{b}^2}{16}\vec{q}^2\right]. \quad (35)$$

C. Numerical results in the two scenarios

In our calculations, $b_N=b_\Delta=0.5$ fm, $b_c=0.45$ fm, $b_c^r=0.45$ fm, and $\tilde{b}=1.2$ fm are taken as inputs. The probabilities in Eq. (16) are $\alpha^2\sim0.31$ and $\beta^2\sim0.69$. The channel wave functions of the $\Delta\Delta$ in both the single $\Delta\Delta$ channel (scenario A1) and the coupled $\Delta\Delta+CC$ channel (scenario A2) approximations are plotted in Fig. 1(a).[1] In terms of the same chiral $SU(3)$ constituent quark model, the wave functions of the $N\Delta$ system with $(I,S)=(1,2)$ can also be obtained by performing a bound-state RGM calculation with a set of model parameters whose values are slightly varied but are still in the reasonable regions. It is shown that in the obtained wave function, the $^5S_2$ component dominates with a fraction of about 94.47%, when the $N\Delta$ system is weakly bound with a binding energy of $\epsilon=0.25$–18 MeV. The wave functions of the D_{12} in the two cases, $\epsilon=0.25$ MeV and 18 MeV, are displayed in Fig. 1(b).

In terms of the wave functions in the A1, A2, and D_{12} cases, the root-mean-square radii (rms) of the d^* and D_{12} can be calculated straightforwardly. The obtained rms's are listed in Table I. From this table, one sees that for the $d^*(2380)$ in scenario A2, its size is small. This is because the fraction of the CC component of the d^* wave function in the coupled channel case is about 0.69. However, for the D_{12}, one finds that its size is rather large. This can be attributed to its weak binding—namely, the energy level of this state is relatively closer to the $N\Delta$ threshold, the system becomes easily to break up, so the N and Δ are "almost free," and the separation between them becomes rather large. The smaller the binding energy is, the larger the size of the system would be.

[1]The wave functions $r\chi(r)$ in Fig. 1(a) are different from those of $r\psi(r)$ in Refs. [25,26] by a factor of $1/\sqrt{4\pi}$ due to the relation $\chi(r)=\psi(r)Y_{00}(\hat{r})$.

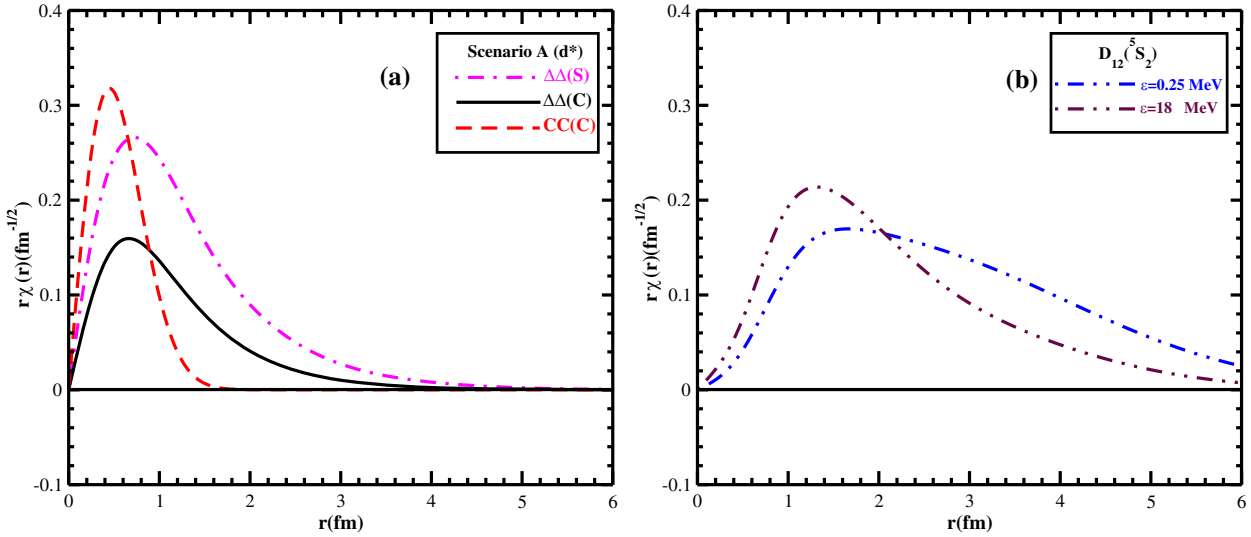

FIG. 1. The wave functions of the d^* and its components in scenario A (a) and of the D_{12} in the $N\Delta$ system (b) in our chiral constituent quark model approach. For the wave functions of the d^* and its components, the pink dashed-dotted curve denotes the relative wave function between Δ and Δ in the single $\Delta\Delta$ channel only [scenario A1 (denoted by "S")], and the black solid and red dashed curves represent the wave functions of the $\Delta\Delta$ and CC components in the coupled $\Delta\Delta + CC$ channel [scenario A2 (denoted by "C")], respectively, in the framework of our chiral $SU(3)$ constituent quark model [25,26]. For the D_{12} wave functions of the $N\Delta$ system, the blue double-dotted-dashed and the maroon double-dotted-dashed curves show the relative wave functions of the $^5S_2$ component in the D_{12}, with the binding energies being $\epsilon = 0.25$ MeV and $\epsilon = 18$ MeV, respectively.

The charge distributions of the d^* in scenario A can be calculated by Eq. (20). The parameters c_m and b_m in Eqs. (21) and (A10) can be found in Refs. [27,28]. The obtained charge distributions from the $\Delta\Delta$ and CC components are demonstrated in Fig. 2. In this figure, the black solid and the red dashed curves denote the contributions from the $\Delta\Delta$ and CC components (scenario A2), respectively, and the black dotted curve represents the total contribution by summing over the former two curves. Here, we only consider the dominanted S-wave component, ignore the small D-wave effect, and normalize the distribution to unity. The charge distribution of the single $\Delta\Delta$ model (scenario A1) is also plotted in Fig. 2 by a pink dotted-dashed curve for comparison. These curves tell us that the contribution from the CC component is larger than that from the $\Delta\Delta$ component, especially in the larger-momentum-transfer region, and the charge distribution of the d^* is dominated by the CC component. It implies that

TABLE I. The calculated rms for the $d^*(2380)$ in the scenarios A1 and A2 and for our D_{12} in the cases B1 and B2, where the corresponding binding energies ϵ are 0.25 MeV and 18 MeV, respectively (in units of fm).

$d^*(2380)$		
Cases	A1	A2
rms (fm)	1.09	0.72
D_{12}		
Cases	B1	B2
rms (fm)	2.64	1.87

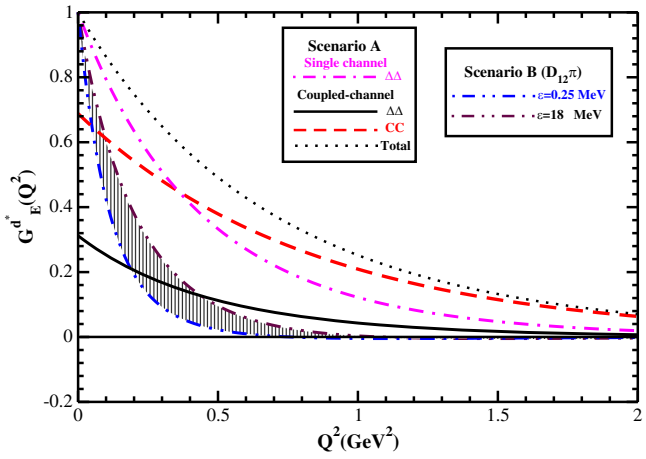

FIG. 2. The obtained charge distributions of the d^* in our chiral constituent quark model. The solid (black), red (dashed), and black (dotted) curves stand for $|\Delta\Delta\chi_\Delta\rangle$, $|CC\chi_c\rangle$, and the *total* contributions in the coupled channel approximation, respectively. The pink dotted-dashed curve represents the single-channel case of scenario A. The blue double-dotted-dashed curve and the maroon double-dotted-dashed curve stand for the results of the $D_{12}\pi$ scenario with $\epsilon = 0.25$ MeV and $\epsilon = 18$ MeV, respectively. The shaded area represents the results with $0.25\ \text{MeV} \le \epsilon \le 18\ \text{MeV}$.

the quark contents in the CC component tend to concentrate in a more compact region than that in the $\Delta\Delta$ component. This physical picture coincides with the radii of the two components of the d^* calculated in our previous papers [25,26]. Moreover, the curvature of the distribution curve in the A1 case is larger than that in the coupled channel case of A2. It indicates that quarks in the former case distribute in a larger region than those in the latter case. The size information of the d^* can also be seen from the slope of the distribution curve at the origin, because such a slope is closely related to the radius of the system. The larger the slope at the origin is, the larger the radius of the system would be. Comparing these slopes with the wave functions shown in Fig. 1(a), we find that the obtained slopes at the origin here coincide with the radii shown in Fig. 1(a). Namely, the radius obtained in the A2 case is smaller than that in the A1 case, and the contribution from the CC component is smaller than that from the $\Delta\Delta$ component.

In order to roughly estimate the size character of the $D_{12}\pi$ structure, the charge distribution of the d^* in this scenario is calculated by using Eq. (34) as well. Notice that since in this case we only consider the contribution from the $D_{12}\pi$ component here, for comparison, we artificially normalize the $D_{12}\pi$ contribution at $Q^2 = 0$ to unity. The obtained charge distribution of the d^* in scenario B is also demonstrated in Fig. 2, where the shaded area between the blue double-dotted-dashed curve and the maroon double-dotted-dashed curve stands for the charge distributions of the $d^*(2380)$ with $0.25\ \text{MeV} \leq \epsilon \leq 18\ \text{MeV}$ in our chiral quark model calculation. We should be aware again that, as mentioned above, we take a relative single P-wave function with a varying size parameter $\tilde{b}$ as a test wave function first. When $\tilde{b}$ takes a value from 0.6–6 fm, the obtained charge distribution of the $D_{12}\pi$ structure only shows a very small variation—namely, this curve is almost insensitive to the size parameter $\tilde{b}$. This is because the incoming photon is absorbed by the D_{12} system, and the induced change of the relative momentum between the D_{12} and π is very small due to the factor of $m_\pi/(M_{D_{12}} + m_\pi) \sim 6/100$. The major influence to the charge distribution comes from the character of D_{12}. Therefore, as a rough estimation in our preliminary study for comparison, we can take a single P-wave function with a $\tilde{b}$ value in the above mentioned region as the relative wave function without strictly solving the $D_{12}\pi$ system but still keep the general character of such a structure.

Comparing the curves in scenario B with the others in scenario A, we see that the curve in the $D_{12}\pi$ scenario decreases and goes to zero much faster than those in scenario A. A much larger slope at the origin means that the radius of the $D_{12}\pi$ system is much larger in comparison with those in scenario A.

From our numerical calculation, we find that the ratios of the slopes of the curves at the origin in scenarios A1 and A2, and in cases B1 and B2, are

$$R = \left[\left(-\frac{\partial G_E^{(A1)}(Q^2)}{\partial q^2}\right)\Big/\left(-\frac{\partial G_E^{(A2)}(Q^2)}{\partial q^2}\right)\Big/ \left(-\frac{\partial G_E^{(B1)}(Q^2)}{\partial q^2}\right)\Big/\left(-\frac{\partial G_E^{(B2)}(Q^2)}{\partial q^2}\right)\right]\Big|_{Q^2=0} = 2.30:1.45:8.70:5.10. \quad (36)$$

It should be mentioned that the contributions from the $\Delta\Delta$ and CC components in the coupled-channel approximation in scenario A2 to $\partial G_E^{(A2)}(Q^2)/\partial q^2$ are 0.64 and 0.81, respectively. As a very rough estimation, we find that the slopes of the charge distribution of the $D_{12}\pi$ structure in the cases B1 and B2 at $Q^2 = 0$ are about $6.0 \sim 3.5$ times larger than that of the d^* in scenario A2. Finally, the very steep charge distribution (or large charge radii) of the $D_{12}\pi$ structure in scenario B (the shaded area between the cases B1 and B2) is mainly attributed to a very extended wave function of the D_{12} obtained in the quark-level calculation. Anyway, a compact structure of the d^* in scenario A2 and a structure of the $D_{12}\pi$ in scenario B (namely, two extreme structures) will give very different descriptions for its charge distribution and its charge radius. The relevant experimental data in the future would be expected to clarify the structure of the $d^*(2380)$.

IV. SUMMARY

Based on our chiral $SU(3)$ constituent quark model, we calculate the charge distributions of the d^* with a hexaquark-dominant structure in scenario A, and that of the d^* with a $D_{12}\pi$ structure in scenario B. In scenario A2, we show the total charge distribution and both contributions from its $\Delta\Delta$ and CC components. In order to make a comparison, the result of the single $\Delta\Delta$ channel is also shown. Comparing the results in scenarios A2 and B, we see that the charge distribution of a $D_{12}\pi$ system is remarkably different from that of a compact structure in scenario A2, and consequentially, the charge radius of the $D_{12}\pi$ in scenario B is obviously larger than that of the compact structure in scenario A2. Finally, it should be reiterated that the present comparison is just a qualitative discussion, because the relative wave function between D_{12} and π is not strictly solved, but the numerical result has shown an insensitivity to the wave function form. In addition, it should be emphasized once more that the concept of the $D_{12}\pi$ structure of the d^* in our calculation is borrowed from Ref. [18]; however, the calculation is in the quark degrees of freedom rather than in the hadron level.

We now expect a series of experiments which may be able to test the different interpretations of the d^* in the future. Although the direct ed^* scattering measurement may be hard to carry out, one may consider the d^* form factors in the timelike region. Moreover, the production of the final $d^*\bar{d}^*$ pair in the e^+e^- and $p\bar{p}$ annihilation processes is also very promising. It is our hope that the

future upgraded BEPC, Belle, and *BABAR* and experiments at $\bar{P}anda$ with high luminosity may provide a platform to test different theoretical understandings.

ACKNOWLEDGMENTS

We would like to thank Heinz Clement, Qiang Zhao, and Qi-Fang Lü for their useful and constructive discussions. This work is supported by the National Natural Sciences Foundations of China under Grants No. 11475192, No. 11475181, No. 11521505, No. 11565007, and No. 11635009, the fund provided to the Sino-German CRC 110 "Symmetries and the Emergence of Structure in QCD" project by NSFC under Grant No. 11621131001, the Key Research Program of Frontier Sciences, CAS, Grant No. Y7292610K1, and the IHEP Innovation Fund Under Grant No. Y4545190Y2. F. Huang is grateful for the support of the Youth Innovation Promotion Association of CAS under Grant No. 2015358.

APPENDIX: d^* IN THE CHIRAL CONSTITUENT QUARK MODEL

The six-quark system with quantum numbers $I(J^P) = 0(3^+)$ is solved in the quark degrees of freedom by employing the chiral $SU(3)$ constituent quark model [34,35]. In this model, the interactive Lagrangian between quark and scalar and pseudoscalar chiral fields is written as

$$\mathcal{L}_I^{\rm ch} = -g_{\rm ch}\bar{\psi}\left(\sum_{a=0}^{8}\lambda_a\sigma_a + i\gamma_5\sum_{a=0}^{8}\lambda_a\pi_a\right)\psi, \quad \text{(A1)}$$

and the interactive Lagrangian between quark and vector meson fields is read as

$$\mathcal{L}_I^{\rm chv} = -g_{\rm chv}\bar{\psi}\gamma_\mu\lambda_a\rho_a^\mu\psi - \frac{f_{\rm chv}}{2M_N}\bar{\psi}\sigma_{\mu\nu}\lambda_a\partial^\mu\rho_a^\nu\psi. \quad \text{(A2)}$$

Then the total Hamiltonian of the system can be found in the form of

$$H = \sum_{i=1}^{6}T_i - T_G + \sum_{j>i=1}^{6}(V_{ij}^{\rm OGE} + V_{ij}^{\rm conf} + V_{ij}^{\rm ch} + V_{ij}^{\rm chv}), \quad \text{(A3)}$$

with $V_{ij}^{\rm ch}$ and $V_{ij}^{\rm chv}$ being the chiral field and vector-meson-induced effective interactions, respectively, between the ith quark and the jth quark,

$$V_{ij}^{\rm ch} = \sum_{a=0}^{8}V_{ij}^{\sigma_a} + \sum_{a=0}^{8}V_{ij}^{\pi_a}, \quad \text{(A4)}$$

and

$$V_{ij}^{\rm chv} = \sum_{a=0}^{8}V_{ij}^{\rho_a}, \quad \text{(A5)}$$

where V^{σ_a}, V^{π_a}, and V^{ρ_a} are the potentials induced by the scalar, pseudoscalar, and vector meson fields, respectively, with T_i being the kinetic energy operator for the ith quark, T_G the kinetic energy operator for the center-of-mass motion of the system, and $V^{\rm OGE}$ and $V^{\rm conf}$ representing the one-gluon-exchange and confinement potentials, respectively. Note that the model that includes the vector-meson-induced potentials is renamed as the extended chiral $SU(3)$ constituent quark model. The parameters of the model are determined by fitting the experimental data of the masses of the ground-state baryons, the phase shifts and cross sections of the NN scattering, the binding energy of the deuteron, etc. The detailed forms of the potentials, model parameter determinations, and resultant values of parameters can be found in Refs. [35,37].

To study the properties of this six-quark system, we proposed a trial wave function in the form of

$$|\Psi_{6q}\rangle = \mathcal{A}[\phi_\Delta(\vec{\xi}_1,\vec{\xi}_2)\phi_\Delta(\vec{\xi}_4,\vec{\xi}_5)\eta_{\Delta\Delta}(\vec{r}) + \phi_{\rm C}(\vec{\xi}_1,\vec{\xi}_2)\phi_{\rm C}(\vec{\xi}_4,\vec{\xi}_5)\eta_{\rm CC}(\vec{r})]_{S=3,I=0,C=(00)}, \quad \text{(A6)}$$

where Δ and C stand for the Δ and hidden color states with the following symmetry and quantum numbers:

$$\Delta:\ (0s)^3[3]_{\rm orb}, S = 3/2, I = 3/2, \qquad C = (00),$$
$$C:\ (0s)^3[3]_{\rm orb}, S = 3/2, I = 1/2, \qquad C = (11).$$

$\mathcal{A}$ is the antisymmetrizer required by the Pauli exclusion principle, $\phi_{\Delta({\rm C})}$ denotes the antisymmetrized internal wave functions of the (123) ((456)) three-quark cluster with $\boldsymbol{\xi}_i$ $[i = 1, 2(4,5)]$ being its internal Jacobi coordinates, and $\eta_{\Delta\Delta({\rm CC})}$ describes the wave function of the relative motion between two $\Delta(C)$ clusters, which is determined completely by the dynamical calculation of the six-quark system.

For a six-quark system, the binding energy relative to the threshold of the $\Delta\Delta$ channel and the corresponding wave function of the relative motion between clusters are obtained by numerically solving the bound-state resonating group method (RGM) equation [25,26],

$$\langle\delta\Psi_{6q}|H - E|\Psi_{6q}\rangle = 0. \quad \text{(A7)}$$

It should be mentioned that RGM is a standard method for few-body physics. For example, there are many calculations for the baryon-baryon interaction by employing this method in the literature [9,15,35,59–68].

Apparently, the obtained wave functions for $\Delta\Delta$ and CC are not orthogonal to each other due to the transition between these two channels, which is caused by quark exchanges. Thus, they cannot be used to distinguish the

components of $\Delta\Delta$ and CC in d^*. Instead, the channel wave functions in the quark cluster model are introduced [69–71], which are orthogonal among various channels. In the present case, the channel wave functions for $\Delta\Delta$ and CC are defined as

$$\chi_{\Delta\Delta}(\vec{r}) \equiv \langle \phi_\Delta(\vec{\xi}_1,\vec{\xi}_2)\phi_\Delta(\vec{\xi}_4,\vec{\xi}_5)|\Psi_{6q}\rangle, \tag{A8a}$$

$$\chi_{\rm CC}(\vec{r}) \equiv \langle \phi_{\rm C}(\vec{\xi}_1,\vec{\xi}_2)\phi_{\rm C}(\vec{\xi}_4,\vec{\xi}_5)|\Psi_{6q}\rangle, \tag{A8b}$$

where $\phi_{\Delta(\rm C)}$ and Ψ_{6q} are the antisymmetrized internal wave function for the cluster of $\Delta(C)$ and the resultant solution of the RGM equation. Then the wave function of d^* can simply be abbreviated and expanded as

$$\begin{aligned}|\Psi_{d^*}\rangle &= |\Delta\Delta\rangle\chi_{\Delta\Delta}(\vec{r})\zeta_{\Delta\Delta} + |{\rm CC}\rangle\chi_{\rm CC}(\vec{r})\zeta_{\rm CC} \\ &= \sum_{L=0,2}\left[|\Delta\Delta\rangle\frac{\chi^L_{\Delta\Delta}(r)}{r}\zeta_{\Delta\Delta} + |{\rm CC}\rangle\frac{\chi^L_{\rm CC}(r)}{r}\zeta_{\rm CC}\right]Y_{L0}(\hat{r}).\end{aligned} \tag{A9}$$

Finally, for easily carrying out analytic derivation in later calculations, the channel wave functions $\chi_{\Delta\Delta(CC)}$ can also be expended by a set of Gaussian functions

$$\chi(r)_{\Delta\Delta({\rm CC})} = \sum_{m=1}^{4}\frac{c_m^{\Delta\Delta({\rm CC})}}{\sqrt{4\pi}}\exp\left(-\frac{r^2}{2(b_m^{\Delta\Delta({\rm CC})})^2}\right), \tag{A10}$$

where $c_m^{\Delta\Delta({\rm CC})}$ and $b_m^{\Delta\Delta({\rm CC})}$ can be determined in the curve fitting process.

[1] M. Bashkanov *et al.*, Phys. Rev. Lett. **102**, 052301 (2009).
[2] P. Adlarson *et al.*, Phys. Rev. Lett. **106**, 242302 (2011); P. Adlarson *et al.*, Phys. Lett. B **721**, 229 (2013); P. Adlarson *et al.*, Phys. Rev. Lett. **112**, 202301 (2014).
[3] A. Abashian, N. E. Booth, and K. W. Crowe, Phys. Rev. Lett. **5**, 258 (1960); N. E. Booth, A. Abashian, and K. M. Crowe, Phys. Rev. Lett. **7**, 35 (1961); F. Plouin *et al.*, Nucl. Phys. **A302**, 413 (1978); J. Banaigs, J. Berger, L. Goldzahl, L. Vu Hai, M. Cottereau, C. Le Brun, F. L. Fabbri, and P. Picozza, Nucl. Phys. **B105**, 52 (1976).
[4] M. Bashkanov, H. Clement, and T. Skorodko, Eur. Phys. J. A **51**, 87 (2015).
[5] COSY confirms existence of six-quark states, CERN Courier **54**, No. 6, 6 (23 July, 2014).
[6] H. X. Chen, W. Chen, X. Liu, and S. L. Zhu, Phys. Rep. **639**, 1 (2016).
[7] J. Dyson, Phys. Rev. Lett. **13**, 815 (1964).
[8] P. J. Mulders, A. T. M. Aerts, and J. J. De Swart, Phys. Rev. D **21**, 2653 (1980).
[9] M. Oka and K. Yazaki, Phys. Lett. **90B**, 41 (1980).
[10] P. J. Mulders, A. T. Aerts, and J. J. de Swart, J. Phys. G **9**, 1159 (1983).
[11] M. Cvetic, B. Golli, N. Mankoc-Borstnik, and M. Rosina, Phys. Lett. **93B**, 489 (1980).
[12] K. Maltman, Nucl. Phys. **A438**, 669 (1985).
[13] R. D. Mota, A. Valcarce, F. Fernandez, D. R. Entem, and H. Garcilazo, Phys. Rev. C **65**, 034006 (2002).
[14] T. Goldman, K. Maltman, G. J. Stephenson, Jr., K. E. Schmidt, and Fan Wang, Phys. Rev. C **39**, 1889 (1989).
[15] X. Q. Yuan, Z. Y. Zhang, Y. W. Yu, and P. N. Shen, Phys. Rev. C **60**, 045203 (1999).
[16] J. L. Ping, H. X. Huang, H. R. Pang, F. Wang, and C. W. Wong, Phys. Rev. C **79**, 024001 (2009).
[17] H. Huang, J. Ping, and F. Wang, Phys. Rev. C **89**, 034001 (2014).
[18] A. Gal and H. Garcilazo, Phys. Rev. Lett. **111**, 172301 (2013).
[19] A. Gal and H. Garcilazo, Nucl. Phys. **A928**, 73 (2014).
[20] A. Gal, Acta Phys. Pol. B **47**, 471 (2016).
[21] A. Gal, EPJ Web Conf. **130**, 01030 (2016).
[22] M. N. Platonova and V. I. Kukulin, Phys. Rev. C **87**, 025202 (2013).
[23] M. N. Platonova and V. I. Kukulin, Nucl. Phys. **A946**, 117 (2016).
[24] M. N. Platonova and V. I. Kukulin, Phys. Rev. D **94**, 054039 (2016).
[25] F. Huang, Z. Y. Zhang, P. N. Shen, and W. L. Wang, Chin. Phys. C **39**, 071001 (2015).
[26] F. Huang, P. N. Shen, Y. B. Dong, and Z. Y. Zhang, Sci. China Phys. Mech. Astron. **59**, 622002 (2016), and references therein.
[27] Y. Dong, P. Shen, F. Huang, and Z. Zhang, Phys. Rev. C **91**, 064002 (2015).
[28] Y. Dong, F. Huang, P. Shen, and Z. Zhang, Phys. Rev. C **94**, 014003 (2016).
[29] Y. Dong, F. Huang, P. Shen, and Z. Zhang, Phys. Lett. B **769**, 223 (2017).
[30] A. Gal, Phys. Lett. B **769**, 436 (2017), and references therein.
[31] The WASA-at-COSY Collaboration, arXiv:1702.07212V1.
[32] M. Bashkanov, S. J. Brodsky, and H. Clement, Phys. Lett. B **727**, 438 (2013).
[33] H. Clement, Prog. Part. Nucl. Phys. **93**, 195 (2017), and references therein.
[34] Y. W. Yu, Z. Y. Zhang, P. N. Shen, and L. R. Dai, Phys. Rev. C **52**, 3393 (1995).
[35] Z. Y. Zhang, Y. W. Yu, P. N. Shen, L. R. Dai, A. Faessler, and U. Straub, Nucl. Phys. **A625**, 59 (1997).
[36] P. N. Shen, Z. Y. Zhang, Y. W. Yu, X. Q. Yuan, and S. Yang, J. Phys. G **25**, 1807 (1999).
[37] L. R. Dai, Z. Y. Zhang, Y. W. Yu, and P. Wang, Nucl. Phys. **A727**, 321 (2003).
[38] Q. B. Li, P. N. Shen, Z. Y. Zhang, and Y. W. Yu, Nucl. Phys. **A683**, 487 (2001).

[39] N. Barik, S. N. Jena, and D. P. Rath, Phys. Rev. D **41**, 1568 (1990).
[40] A. W. Thomas and W. Weise, *The Structure of the Nucleon* (WILEY-VCH Verlag, Berlin, 2001).
[41] P. Mergell, U. G. Meissner, and D. Drechsel, Nucl. Phys. **A596**, 367 (1996).
[42] J. J. Kelly, Phys. Rev. C **66**, 065203 (2002).
[43] S. Pacetti, R. Baldini Ferroli, and E. Tomasi-Gustafsson, Phys. Rep. **550–551**, 1 (2015).
[44] M. V. Galynskii and E. A. Kuraev, JETP Lett. **96**, 6 (2012).
[45] R. G. Arnold, C. E. Carlson, and F. Gross, Phys. Rev. C **23**, 363 (1981).
[46] M. Garcon and J. W. Van Orden, Adv. Nucl. Phys. **26**, 293 (2001).
[47] E. Tomasi-Gustafsson, G. I. Gakh, and C. Adamuscin, Phys. Rev. C **73**, 045204 (2006).
[48] Y. B. Dong, A. Faessler, T. Gutsche, and V. E. Lyubovitskij, Phys. Rev. C **78**, 035205 (2008).
[49] S. Boffi, C. Giusti, F. D. Pacati, and M. Radici, *Electromagnetic Response of Atomic Nuclei* (Clarendon Press, Oxford, 1996).
[50] F. Cardarelli, I. L. Grach, I. M. Narodetsky, G. Salme, and S. Simula, Phys. Lett. B **349**, 393 (1995).
[51] J. P. B. C. de Melo and T. Frederico, Phys. Rev. C **55**, 2043 (1997).
[52] H. M. Choi and C. R. Ji, Phys. Rev. D **70**, 053015 (2004).
[53] B. D. Sun and Y. B. Dong, Phys. Rev. D **96**, 036019 (2017).
[54] T. M. Aliev, K. Azizi, and M. Savci, Phys. Lett. B **690**, 164 (2010).
[55] R. D. Mota, A. Valcarce, F. Fernandez, and H. Garcilazo, Phys. Rev. C **59**, 46 (1999); **65**, 034006 (2002).
[56] T. Kamae and T. Fujita, Phys. Rev. Lett. **38**, 471 (1977).
[57] C. Heon Oh, R. A. Arndt, I. I. Strakovsky, and R. L. Workman, Phys. Rev. C **56**, 635 (1997).
[58] S. R. Amendolia *et al.*, Nucl. Phys. **B277**, 168 (1986).
[59] K. Wildermuth and Y. C. Tang, *A Unified Theory of the Nucleus* (Academic Press, New York, 1977).
[60] J. E. T. Ribeiro, Z. Phys. C **5**, 27 (1980).
[61] M. Oka and K. Yazaki, Prog. Theor. Phys. **66**, 556 (1981).
[62] A. Faessler, F. Fernandez, G. Lubeck, and K. Shimizu, Phys. Lett. **112B**, 201 (1982).
[63] A. Faessler, F. Fernandez, G. Lubeck, and K. Shimizu, Nucl. Phys. **A402**, 555 (1983).
[64] M. Oka and K. Yazaki, *Quarks and Nuclei*, edited by W. Weise (World Scientific, Singapore, 1984), p. 489.
[65] A. Faessler, Prog. Part. Nucl. Phys. **11**, 171 (1984); **13**, 253 (1985); **20**, 151 (1988).
[66] K. Shimizu, Rep. Prog. Phys. **52**, 1 (1989).
[67] Y. Yamauchi, K. Tsushima, and A. Faessler, Few-Body Syst. **12**, 69 (1992).
[68] M. Lacombe, B. Loiseau, R. Vinh Mau, P. Demetriou, J. P. B. C. de Melo, and C. Semay, Phys. Rev. C **65**, 034004 (2002).
[69] A. M. Kusainov, V. G. Neudatchin, and I. T. Obukhovsky, Phys. Rev. C **44**, 2343 (1991).
[70] L. Ya. Glozman, V. G. Neudatchin, and I. T. Obukhovsky, Phys. Rev. C **48**, 389 (1993).
[71] Fl. Stancu, S. Pepin, and L. Ya. Glozman, Phys. Rev. C **56**, 2779 (1997).